Journal of Brilliant Engineering 3 (2022) 4683
Brilliant Engineering
journal home: www.acapublishing.com/journals/4/ben

Research Article

Optimization of Load Values in Pipe Hydroforming Process Using A Fuzzy Load Control Algorithm

Vahid Jafarpour [*,1], Maryam Abasi [2]
[1]Department of Mechanical and Aerospace Engineering, University of Texas at Arlington, Texas, USA
[2]Department of Mechanical Engineering, Lamar University, Texas, USA

Keywords

Pipe hydroforming,
Optimal loading path,
Optimization,
Fuzzy control.

Abstract

One of the most advanced methods of metal shaping techniques is hydroforming, which uses fluid at extreme pressure to deform metal sheets that cannot be fabricated by conventional approaches. This method is perfect for the production of lightweight, seamless, continuous, mesh-shaped, high-quality, and important high-strength automotive and aircraft components. When it comes to pipe hydroforming, the ductility of the metal pipe has a direct impact on the forming load route. (Internal deformation pressure and axial feeding). This research focuses on the impact of operational circumstances. (i.e., the impact of ultimate longitudinal feeding and forming pressure) on the whole procedure and keeps the other factors fixed. The control algorithms were designed to control longitudinal feeding and pressure over the shaping process modeling. Most of the pipe hydroforming paths are created during the multi-stage procedure for loading. Hence the deformation limit strains obtained in the middle of the deformation procedure depend on the route. The present work optimizes the loading path angles in the pipe deformation procedure using an intelligent algorithm for fuzzy logic control. This prevents the tube from breaking or rupturing during the forming process due to high strains. The mentioned control algorithm and fuzzy adaptive neural system (ANSYS) were used to simulate the hydroforming procedure.

1.Introduction

Optimization has gotten a lot of attention in the manufacturing areas. Huge amounts of work have been done to reach the optimum results using either experimental or numerical analyses to deracease the overall costs and improve the process, efficiency, and accuracy[1-2]. To handle the challenges, intelligent optimization algorithms and their updated variants such as genetic algorithms, differential evolution, adaptive Neuro-fuzzy system(ANFIS)and Taguchi techniques are introduced[3-5]. As a salient example, Chen et al. improved the turning method to increase machining efficiency. The implementation of PSO's optimization procedure boosted machining efficiency by roughly 8%[6]. Jafarpour et al. (2022)[7] optimized the creep-feed grinding process using a finite-element model to reach the best possible machining efficiency. One of the most sophisticated metal shaping technologies is hydroforming, which uses high-pressure fluid to deform metal sheets that cannot be fabricated by conventional procedures. This procedure is perfect for the production of lightweight, seamless, continuous, mesh-shaped, high-quality, and important high-strength automotive and aircraft components. Because of the cost advantages of this manufacturing process, the automotive and aircraft industries have recently implemented it in production worldwide. Recent advances in FEM have led to the modeling of the majority of the hydroforming procedures. In the present work, the tubular deformation procedures X and T-shape are modeled and the best loading routes are acquired for such operations.

The product of the hydroforming procedure is determined by several variables that have a fundamental impact on the procedure. Such factors may be categorized as operational circumstances; material characteristics, geometrical profile, and loads of the workpiece [8]. This study focuses on the impact of operational circumstances. (i.e., the impact of ultimate longitudinal feeding and forming pressure) on the whole procedure and keeps the other factors fixed. The control algorithms were designed to control longitudinal feeding and pressure over the shaping process modeling. A similar effect has been mentioned by Kosters et al. (1998)[9], in which modeling is performed to form a symmetrical tube featuring a longitudinal feeding at the end (a hollow rod is modeled). Miyamoto et al. (2003)[10] also modeled the hydroforming procedure of the T-shaped pipe and to regulate the final longitudinal feeding, employ fuzzy adaptive process control, in which the inner deformation pressure was measured separately. implemented. During their research, they used pipe buckling as the main criteria of failure and based on it, fuzzy control operation was developed. R. Mayey et al. (2009)[11] used the LS-DYNA code in finite element simulation and experimental work to optimize the hydroforming piping process. Their objective was to enhance ductility by identifying optimal pressure rates and axial feeding. In this case, the fracture range was characterized by the forming limit diagram (FLD). The optimal values obtained in the simulation and experimental work results are well consistent and within the safe range of the shaping limit diagram. S. Memon et al. (2013)[12] optimized the symmetrical hydroforming of the pipe to achieve maximum bulge, without fracture and rupture in the deformed part. The effect of strain path and its relationship with bulge height was also investigated. In this study, the Taguchi analysis technique was employed to enhance process parameters. The results of their work in optimizing the process parameters were not only reaching a higher peak height and less thinning but also a uniform deformation pattern (effective strain and thinning) was obtained. Yaghoobi, et al. (2016) [13] conducted a study in 2013 on the use of a fuzzy adaptive neural system (ANFIS) and genetic algorithm (GA) to optimize the pressure route in the sheet hydroforming procedure. The ANFIS model was developed in this work based on FEM outcomes to determine the pressure route's influence with the most thinning possible in the sensitive area. The result shows that the combination of the fuzzy adaptive neural system and the optimization algorithm is a suitable scheme for predicting the route of least resistance to loading,

*Corresponding Author: vxj0203@mavs.uta.edu
Received 19 May 2022; Revised 06 June 2022; Accepted 08 June 2022
https://doi.org/10.36937/ben.2022.4683

preventing thinning in the sensitive area of the component, and avoiding simulation or experimental error and multiple tests. In this paper, the mathematical model has been confirmed using the experimental results obtained in the work of Mr. Ray et al. (2005)[14]. In the above-mentioned research work, the hydro-forming procedure of T- and X cross-sectional tubes have been investigated in this research.

The aim of the present study is to figure out the best loading routes using FEM and loading algorithms for T and X cross-sectional tube hydro-forming procedures by maximizing the section peak height and at the same time preserving the thickness of the sidewalls and creating the plastic strains and stresses in the permitted areas. How to figure out the best loading parameters for each hydro-forming procedure including the final axial feeding and the internal pressure, can be described by employing FEM, load control system, and Figure (1). The intelligent fuzzy control algorithm was designed and incorporated with the FEM in the modeling. The algorithm was created utilizing the ANSYS -LS -DYNA design language with parameters.

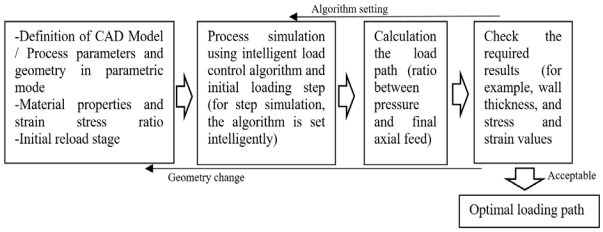

Figure 1. Diagram of determining the optimal loading path using simulation

2. The loading controlling algorithm

The following portion describes the evolution of the adaptive loading management algorithm.

2.1 Controlling the procedure limitations

To be able to successfully apply the hydro-forming procedure of the pipe, prior knowledge of the proper loading route is especially noteworthy. The major failing of the hydro-forming procedure, which results in shrinkage, buckling, or bursting, depends on the final axial feed. In these processes where the wall thickness is not considerable, in case the axial feeding is excessive in terms of interior pressure applied, the possibility of shrinkage is not negligible, which results in buckling. Finally, if the pressure is significant in terms of axial feeding, the bursting of the pipe due to its thinness will be avoidable. Therefore, the hydroforming load needs to be properly adjusted and changed for the process to run successfully. A loading control strategy has been formulated based on these principles. The FEM formulation provides reliable results for predicting buckling and overflowing circumstances [9].

The philosophy behind the load controlling algorithm's development to recognize the origins of buckling or shrinkage of the pipe over FEM is the following paragraphs. Whenever shrinking happens, or the pipe is subject to bursting, the elements of the area under the shrinkage are drawn on the periphery (ε11) and surfaces (ε15) of the interior (Figure.2) respectively. The numerical difference (ε11-ε15=Δε)between these two strain values corresponds to the degree of curvature in a given region. In addition, the vertical velocity (Vn) of the components might be utilized. to determine the desirability of shrinkage, the contact time of the material with the surface of the mold, or to determine whether the shrinkage is a fragile curvature because of the low feed axis or high feed axis. Figure 3 depicts the distinction between the two conditions as stated by the difference in strain (ε) as well as the distribution (Vn).

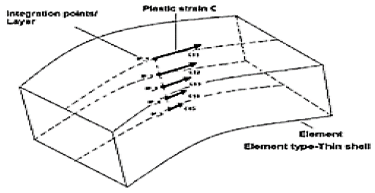

Figure 2. Distribution of strain throughout the element's thickness

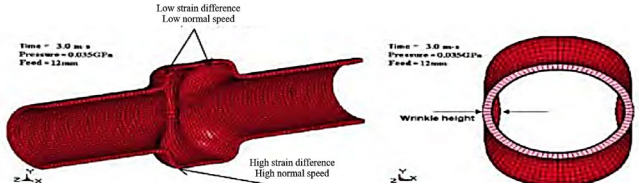

Figure 3. The wrinkled pipe's strain differential and normal speed

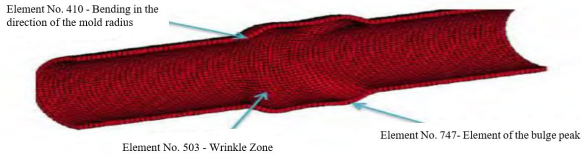

Figure 4. A view of the number of critical elements on the surface of the pipe

Excess compressed material in the forming area may lead to buckling or even greater sidewalls' thickness in some regions. Therefore, it is possible to predict the formation of wrinkles employing a smart controller parameter and to control it in finite element simulation. The load controller parameters attempt to yank the axial feeding as far as possible to the end of the tube and at the same time keep the internal pressure low to avoid bursting, buckling, or shrinking. When it comes to T and X cross-sectional tubes hydro-forming, This controlling method has the potential to adjust as a prerequisite to maximize peak height and maintain maximum tension and thickness within certain ranges.

2.2 Algorithm for controlling loading layout

Figure.5 demonstrates the difference in axial strain on the thickness of the pipe wall during the shaping process for different components. The wrinkled and non-wrinkled regions of the chosen tube are used to create these pieces. (Figure.4) to discriminate between wrinkled and non-wrinkled areas in terms of strain differential and normal velocity changes. Initially, (t =0) for all components, the differences in strain (Δε) are within the acceptable range, and the strain differential for some unstable components slowly increases as time passes (elements 503 and 747), which denotes the occurrence of wrinkles. The normal velocities (Vn) of the elements must be examined to distinguish wrinkle creation from strain differential values. The variation in normal velocity is depicted in Figure 6. (element) of the surface in proportion to the elements having a high strain (elements 503 and 747). Initially, when t =0 , the normal velocities are low, but as time goes on, this parameter increases rapidly, indicating the formation of wrinkles (for example, high strain differences as well as high normal velocities). In element 410, according to the strain and speed diagrams, It has been noted that Although the strain is considerable, the speed is minimal, and therefore under these conditions, the natural curvature of the pipe wall appears across the radius of the mold (Figure 4-6). Hence, in modeling the hydro-forming procedure, two expressions a) the difference in a strain of the element and b) the

normal velocity of the element, outline the emergence of wrinkles or buckling of the part. During the modeling, some components may be pulled hard and the surface speed may be quite considerable, however, this does not rule out the possibility of shrinkage. If wrinkle formation is involved, it begins with a tiny segment, and a modest number of components growing gradually. As a result, determining the part where the wrinkles first appeared is required. When it comes to hydro-forming X and T cross-sectional, pipes, the pipe's surface deformation begins in X or T sections and bends in the mold's radius. Therefore, determining whether the surface of the tube is due to curved wrinkles or the geometry of the mold is a relatively difficult task. Therefore, to assess the potential of shrinkage and the likely regions, in the algorithm, parameter A, which is equal to the value of *Ncse / Ntotal*, is used. Where the number of elements in the component is denoted by Ncse, where the difference in strain (Δε) on the wall thickness of the pipe is greater than the critical value.

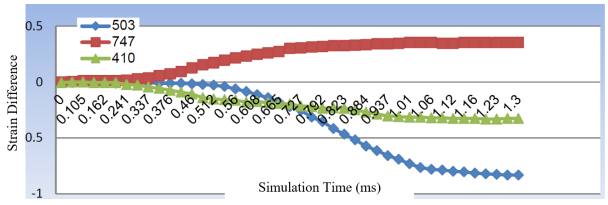

Figure 5. Changes in the strain difference of the element in terms of simulation time (Wrinkled hydro-forming tube)

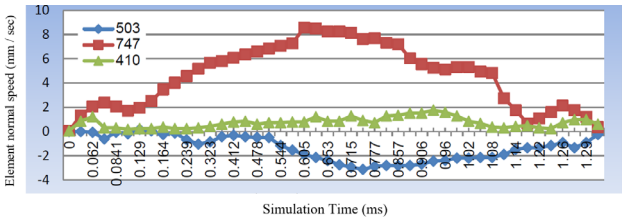

Figure 6. Normal velocity changes of the element in terms of simulation time (wrinkled hydro-forming tube)

Ntotal is the total number of all elements, which is a separate model segment. These pieces were parametrically characterized in FEM. By comparing and contrasting the parameters Δε (difference in strain), Vn (normal speed), and A (relative number of elements under tensile stresses in a particular segment) and proper control can avoid fracture due to buckling or shrinkage during the simulation. In the load control algorithm, the values of the above parameters are employed as input and data. The distinction between the simulation and the applications of traditional control is obtained values during the modeling. The normal velocity numbers vary because of the strain differential and the dynamic nature of the operation is kept oscillating or changing during the whole simulation process (Figures 5 and 6). Therefore, for diverse geometries, quantifying the vital or non-vital states of deformation or wrinkle creation is problematic. Hence, the exact value definition, which indicates the occurrence or non-occurrence of wrinkles, is omitted here. Instead of answering the question of whether wrinkles occur during the shaping process or not, criteria with fuzzy terms and rules are used for evaluation. The basic fuzzy principles are a straightforward logical concept built on the "IF 'X' and 'Y' then 'Z' " strategy which is used for solving the main control problem, instead of mathematical modeling of the system, X and Y are two separate inputs, The consequence or output of the inputs is Z. As a result, the appearance of wrinkles, in this circumstance, logical rules, and language terminology can be used to describe the situation; for instance, "If part of the surface of the pipe bends sharply and the surface moves rapidly the surface bends around the entire radius and in the vertical direction, then severe wrinkles occur." Of course, to define the factors that cause wrinkles to appear or tubular buckling, the parameters are expressed as a difference in strain Δε, normal surface speed (Vn), and parameter A, so that, "Critical and severe wrinkles arise when the absolute amount of difference in strain in a given fragment is very high, the absolute amount of the normal velocity is considerable, and the elements' number is more than the shear strain state in that fragment.". Similarly, the final axial feeding and pressure are figured out. For instance, "in case critical wrinkles occur, the axial feeding should be reduced to the minimum amount and the internal pressure should be increased to the maximum". Also, to prevent bursting fracture, a straightforward zone based on the maximum stress limit is defined, and if the stress is higher than a certain limit, the pressure decreases, and the axial feeding stops; although the above fuzzy expressions are inaccurate, they describe what happens well.

2.2.1 Fuzzification

Before logical rules were included in the control system, variables and input parameters are considered fuzzy. Three categories of regulations were identified: a) Δε (3 categories), b) Vn (3 categories), and c) the number of parts having three separate strain differential categories (3 categories). 27 fuzzy rules are activated by all of these inputs, which justifies the high, medium, or low axial power supply and internal pressure. The program calculates axial feeding values and internal pressure for each piece of the FEM model. Only three separate domains or groups of each input variable are employed to keep the procedure simple, although as the number of groups grows, the control algorithm can get more sensitive and better. Eventually, the output must be defuzed. (Δp and Δd) are calculated by the output set's primary axis. With the diffusion parameters in place, only minor or moderate shrinking is permitted by the process control system throughout the modeling. The control algorithm's fuzzy principle matrix is depicted in Table 1. Likewise, three sets of laws are formed for $a2 \leq A$ and $a1 \leq A \leq a2$, in which the values (pretty low, low, regular, high, and pretty high) are considered as a collection of pressure output membership functions and axial feeding [15].

Table 1. Difference matrix using fuzzy principles for tensile force against normal intensity [15]

Fuzzy load control algorithm ($A \leqslant z1$)	$\Delta\varepsilon$ = abs(+ve high)	$\Delta\varepsilon$ = abs(medium)	$\Delta\varepsilon$ = abs(−ve high)
V_n = abs(+ve high)	Δp = very low(z1) Δd = low(z1)	Δp = low(z1) Δd = normal(z1)	Δp = normal(z1) Δd = normal(z1)
V_n = abs(medium)	Δp = low(z1) Δd = high(z1)	Δp = normal(z1) Δd = very high(z1)	Δp = high(z1) Δd = high(z1)
V_n = abs(−ve high)	Δp = normal(z1) Δd = normal(z1)	Δp = high(z1) Δd = normal(z1)	Δp = very high(z1) Δd = low(z1)

2.2.2 Membership function calculation

A graph representation of the size and presence of each input is considered the membership function, which includes the evaluation of each input and defines all the functional overlays among inputs, and generates the output replies in the end. The working principles are based on determining input membership values as assessment factors of the final results after examining their impact on fuzzy output sets. Here, for the sake of computation simplicity, although the Gaussian or Sigmoid function can also be employed, the fuzzy membership function is defined by sets of linear functions. The formulation of the membership function for surface normal velocity/difference in strain (membership function input) and axial feed and progressive pressure (membership function output) is demonstrated in Figures 7 and 8. The total range of surface velocities and differences in strain is split into three distinct zones. The function of membership for normal speed and negative stress differential is defined in the left half, The function of membership for normal speed and strain differential is defined in the center section (mean), and The function of membership for normal speed and positive strain differential is defined in the right part. Likewise, the axial pressure and feed membership function is split into five distinct regions, i.e. pretty low, low, regular, high, and pretty high.

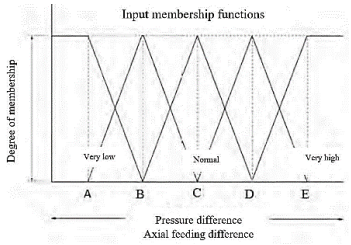

Figure 7. Input degree of membership

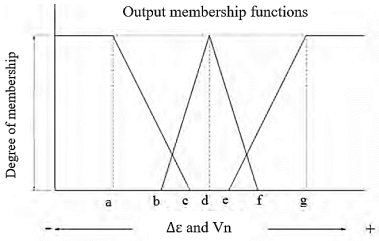

Figure 8.Output degree of membership

2.2.3 Defuzzification and fuzzy results

Finally, the result was defuzzified to calculate the values of effective pressure or axial feeding and to figure out the efficacy of the fuzzy principles. The root-squared sum approach is utilized to defuzzify in this study. The fuzzy center of the composite region is calculated using this method. To address all of the corresponding ideas, the root-squared sum approach was adopted. The algorithm for fuzzy load control and its details in FEM can be observed in the flowchart in Figure (9). The merits of utilizing this kind of monitoring system would be that the normal speeds of the elements are automatically altered as preconditioning in the simulation, and the final axial pressure and feed are adjusted to prevent fracture due to shrinkage, and buckling, or bursting of the pipe. Avoid the length of the shaping process and achieve an optimal loading path.

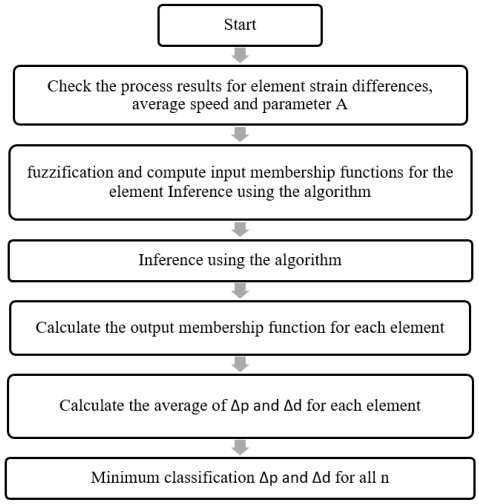

Figure 9. Details of the FEM's fuzzy load control algorithm

3. Employing a controlling algorithm to find the best load route in hydro-forming processes of the T and X cross-sectional tubes

3.1 FEM in T and X cross-sectional tubes deformation procedures

The ANSYS -LS-DYNA specification FEM is used in the simulation of hydroforming processes of pipe having X branch (Figure 10) and T branch (Figure 11). Copper pipe with 24 millimeters (diameter of the outside), 121 millimeters (length), and 1.3-millimeter thickness is employed as the raw material, [14]. Internal hydraulic pressure and axial compressive load are used to compute forming forces. Given the symmetry advantage, the modeling was performed as a quarter of the T-branch and an eighth of the X-branch, respectively [9]. The mold has a variable radius at the intersection, for example, the radius changes from 3 mm (above the curvature of the mold) to infinity (at the edge of the junction of the two cavities). The model and mold mesh in a finite element tube with four 3D thin shell quadratic.

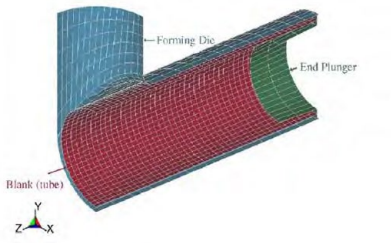

Figure 10. Model FEM of the X-branch of the tube and mold shape

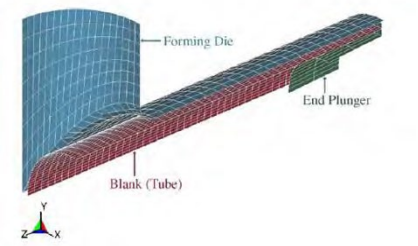

Figure 11. Model FEM of the T-branch of the tube and mold shape [14]

Mold molding is divided into three different regions according to geometry, and the following hypotheses are considered: a) the nature of the mold surface is stiff and b) The linear elastic law governs the mold type. The Belytschko-wong-Chiang element formula was used to create four 3D thin shell explicit nodes, each with five connection points (Figure 2). Five merge point in each node acts as a layer for the shell elements. To calculate the difference in the strain of the element in terms of thickness, the difference between the strain values of the internal and external integration points was obtained. To shorten the simulation duration, the tube's element divisions were designed so that the change in results is confined to a small proportion of the real result and the simulation work is completed with an appropriate number of elements. Finite element models were utilized in conjunction with the algorithm in the parametric form in the ANSYS-LS-DYNA language to establish the ideal loading conditions. The surface-to-surface contact algorithm was used to model the interaction between the tube and the mold. The elastic friction between the pipe and the mold was calculated to have a coefficient of friction of 0.1. Characteristics of the elastoplastic material used within the tube: annealed copper, Yang modulus of 119.86 Gpa, Yield strength of 0.116 Gpa, Poisson's ratio of 0.3, tangent modulus of 0.112 Gpa, Density of 8900 kg / mm and Final tensile strength of 0.330 Gpa [14]. The wall thickness reduction was limited to 0.85 mm, and the modeling began with initial (small-scale) internal hydro-forming pressure and final axial feeding, with the load control algorithm calculating the succeeding pressure and axial feeding amounts.

3.2 Results and Discussion

Because one-quarter of the X-shaped branch and one-eighth of the T-shaped branch are modeled, utilizing the symmetry, the FEM model pipe nodes are tied in the proper directions to maintain symmetry. The A pressure load was applied to the inside surface of the pipe (surface elements) The axial load fed the nodes attached to the pipe's end surface elements as the final feed. The pipe's end surfaces are put on a pin during the actual hydroforming process. The punch isn't modeled in this situation, Instead, the radial and circumferential directions of the nodes on the surfaces of the tube's ends are restricted. The whole process was simulated separately during the five stages and at every step, Depending on the results of the preceding modeling step's strain, stress, and normal velocity values, the fuzzy load control scheme adjusted the axial pressure and feeding

as a precondition. The load proposed controller is a control system that operates in a closed loop that regulates axial pressure and feeds while also preventing wrinkling, buckling, and pipe breaking. Figures 12 and 13 depict the best loading pathways (internal pressure versus axial feeding) for X-shaped and T-shaped hydroforming pipes created during FEM based on the fuzzy loading control algorithm. Figure 14shows the stress distribution in the T-shaped hydroforming pipe during the last stage of modeling. The stress's greatest value is less than the fracture stress (final stress). To ensure that the results are accurate, the strain difference profiles of the element (Figure15) and the normal velocity (Figure16), during the non-wrinkled X-shaped cylinder's whole simulation period hydroforming tube, were matched to the profile of strain differences and the normal velocity of the wrinkled X-shaped tube which can be seen in Figures 4-6. Here, three elements were selected from the critical deformed regions and their velocity patterns and strain differential were investigated. It has been discovered that throughout the simulation procedure (using the load control algorithm), the values of differences in strain are less than the limiting factor of ±18.In element 394, which is subject to curvature along the mold radius, it has a high strain difference (for the modeling time of 0.6 ms until the process is completed), which, of course, is the normal velocity during the process. The surface of the tube has a normal curvature, as evidenced by this, and allows the appearance of wrinkles within the radius. In element 792, to some extent, the strain differential is heightened, albeit somewhat less than the specified shear limits. Of course, the normal velocity is very high throughout the simulation time, which means that the part is exposed to free formation without any wrinkles. The optimal loading path (Figure 12) for the X-shaped branch in the hydroforming simulation was compared to an approximate load path using the loading control methodology. Table 2 shows the research of Ray et al. [7] and Figure 17 shows the results of the two loading routes according to Mc. Donald's research [9 and 16].

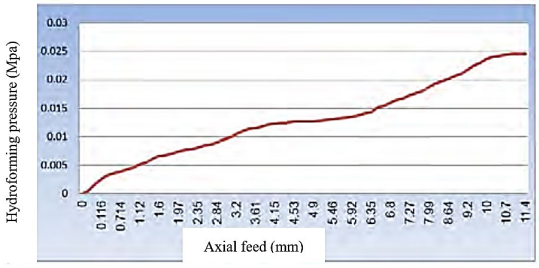

Figure 12. Optimal loading path in X cross-sectional branch hydro-forming

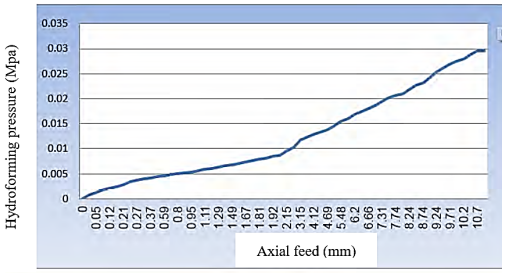

Figure 13. The best loading route in T cross-sectional branch hydro-forming.

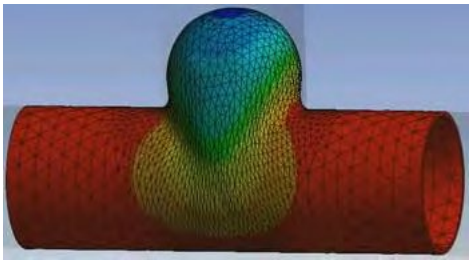

Figure 14. Stress distribution according to Von Mises in the T cross-sectional branch

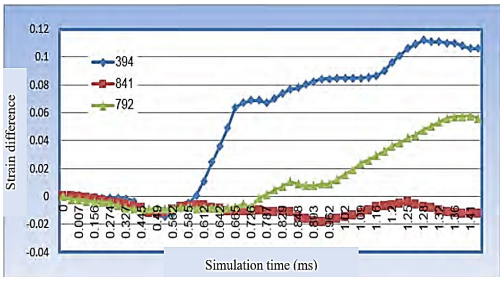

Figure 15. Changes in the strain difference of the element in terms of simulation duration (hydro-forming tube without shrinkage)

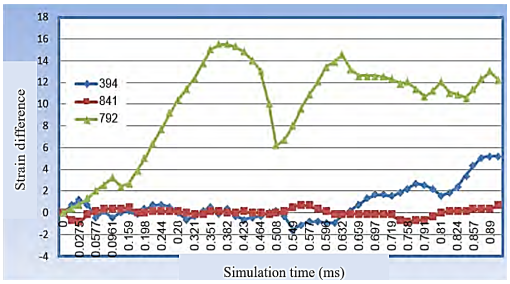

Figure 16. Changes in the normal velocity of the element in terms of simulation duration (hydro-forming tube without shrinkage)

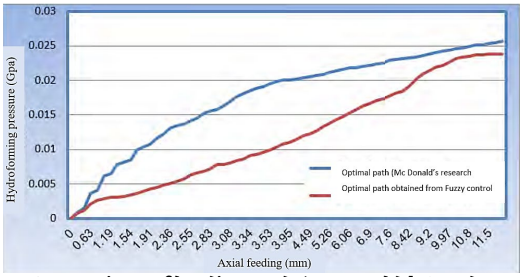

Figure 17. Comparison of loading path (McDonald [16 and 17 and] and fuzzy control for hydro-forming X tube).

Table 2. Comparison of results for X cross-sectional branch pipe hydro-forming

	Ray Results[14]	Simulation results
Maximum axial feeding (mm)	18.5	17.8
Maximum pressure(Gpa)	0.0284	0.0250
Maximum height of the bulge(mm)	14.75	13.9
The final thickness of the bulge's highest point (mm)		1.02

Examining the loading routs, it has been noted that, towards the end of the modeling process, the values of displacement and the pressure in the two routes are nearly identical. The idea proposed by Manabe can explain the variance in the middle portion [10]. For example, in the direction of hydroforming or the successful creation of an X or T branch, the procedure must take place in a specific process network (Figure 18Lastly, the distribution of pipe wall thickness in three planes along the pipe's curved lines was investigated. The wall thickness changes are within the specified 0.86 mm range (from the end of the pipe to the center of the pipe). Thus, the hypothesis that the deformation of the piece in the absence of shrinkage is maximized and the wall thickness is maintained at the same time and the material fed from the end of the pipe is used to increase the height of the branches is proved. Figure 19 depicts a contrast between incensement in-branch thickness and material feeding over time for X- shaped branch hydro-forming. The fact that the two diagrams are identical proves that the material fed from the end of the pipe is used to increase the height of the branch, and it is obvious that the increase in the top of the pipe is maximized and at the same time the wall thickness is maintained. Experiments were performed on a hydroforming tube, the T-shaped directed tube in the work of Ray et

al. Details of the experiment and the results can be seen in Table 3. The path derived from the FEM T-shaped modeling is consistent with the loading route employed in the experiment. The thickness profile in the FEM and the experimental sample are displayed in cross-sections in Figures 18 and 19.

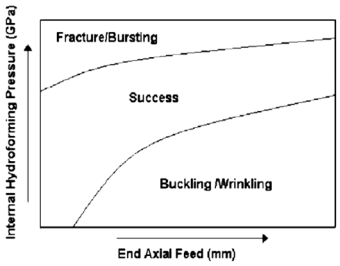

Figure 18. Forming process network for pipe hydroforming in T and X shaped mode [10]

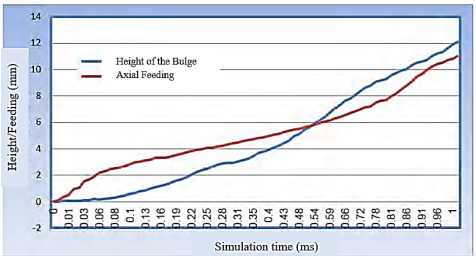

Figure 19. Comparison of X-shaped branch height and axial feeding in terms of simulation duration

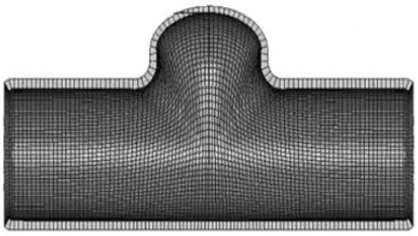

Figure 20. FEM of the hydro-forming tube (T-shaped) along with the wall thickness

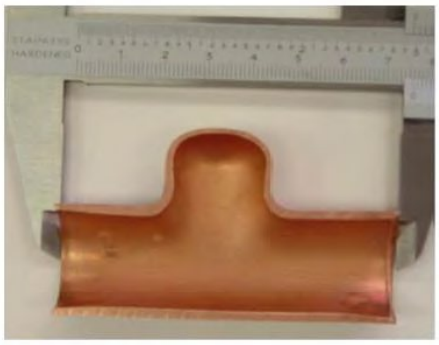

Figure 21.Hydroformed tube cross-section (T-shaped)

4. Conclusion

Using the smart load control technique based on fuzzy logic, the optimal loading paths in the hydroforming procedure for asymmetric tubes (X and T shaped branches) were decided in this research. The control and maximum branch height algorithm were used to forecast the load path for the X-shaped branch, which agrees well with the load route employed and the results provided by McDonald. et al. [9 and 10]. In addition, the load route generated by the T-shaped branch simulation and the experimental data reported by Ray et al are aligned. During the modeling, the algorithm functions as a closed-loop controlling system, monitoring pressure, feeding, and preventing fractures due to shrinkage, buckling, or bursting. The distinction between traditional FEM control and modeling with the control algorithm is that in the FEM process, the values of incremental pressure and ultimate axial feeding of hydroforming are acquired. The algorithm can be utilized to discover the ideal load routes for shaping asymmetric and symmetrical axes with very complex geometries by slightly adjusting the strain range settings (according to application, material type, thickness, and pipe diameter) in the load control algorithm.

Declaration of Conflict of Interests

The author declares that there is no conflict of interest. They have no known competing financial interests or personal relationships that could have appeared to influence the work reported in this paper.

References

[1.] Jafarpour, V. and Moharrami, R., Experimental Study on In-Depth Residual Stress due to 420 Stainless Steel Creep-Feed Grinding Using the Deflection-Electro Polishing Technique. *Journal of Modern Processes in Manufacturing and Production,* 2022.11(1):p. 59-74. https://dorl.net/dor/20.1001.1.27170314.2022.11.1.4.0

[2.] Moharrami, R. and V. Jafarpour. Experimental Study of Residual Stresses Due to Inconel X-750 Creep-feed Grinding by the Electro polishing Layer Removal Technique. Journal of Stress Analysis. 2019.4:p. 65-71. https://dx.doi.org/10.22084/jrstan.2019.19668.1098

[3.] Thepsonthi, T. and O¨ zel, T., Multi-objective process optimization for micro-end milling of Ti-6Al-4V titanium alloy. Int J Adv Manuf Technol,2012.63:p.903–914.

[4.] Li, C., et al., Selection of optimum parameters in multi-pass face milling for maximum energy efficiency and minimum production cost. J Clean Prod, 2017.140(3):p.1805–1818.

[5.] Jafarpour, V., Parameter Optimization of Spot-Welded Aluminum Plates Using the Adaptive Neuro-Fuzzy System with Genetic Algorithm. Mapta Journal of Mechanical and Industrial Engineering (MJMIE),2022.6(01):p.10–17.

[6.] Chen, D., et al., Study on the optimization of cutting parameters in turning thin-walled circular cylindrical shell based upon cutting stability. Int J Adv Manuf Technol,2013.69:p.891–899.

[7.] Jafarpour, V. and Moharrami, R., Numerical Stress Analysis of Creep-Feed Grinding Through Finite Element Method in Inconel Alloy X-750. Mapta Journal of Mechanical and Industrial Engineering (MJMIE),2022.6(01):p.1–9.

[8.] Rimkus, W., et al., Design of load curves for hydroforming application. J. Mater. Process. Technol, 2000.108:p.97–105.

[9.] Doege, E., et al., Determination Of Optimised Control Parameters For Internal High Pressure Forming Processes With The FEM, Proceedings of the International Conference Sheet Metal'98 ,1998:p. 119–128.

[10.] Manabe, K., et al., Application of Database-Assisted Fuzzy Adaptive Process Control System to Hydroforming Process. Intelligence in a Materials World—Selected Papers from IPMM-2001 CRC Press ,2003:p. 537–543.

[11.] Abedrabboa, N., et al., Optimization Methods For The Tube Hydroforming Process Applied To Advanced High-Strength Steels With Experimental Verification. journal of materials processing technology,2009(209):p.110–123.

[12.] Memon, S., et al., Finite Element Analysis For Optimising Process Parameters in Tube Hydroforming Process. IDDRG 2013 Conference.

[13.] Yaghoobi, A., et al., Application Of Adaptive Neuro Fuzzy Inference System And Genetic Algorithm For Pressure Path Optimization In Sheet Hydroforming Process. The International Journal of Advanced Manufacturing Technology, 2016:p.1-11.

[14.] Ray, P., et al., Experimental Study and Finite Element Analysis of Simple X- And T-Branch Tube Hydroforming Processes. International Journal of Mechanical Sciences, 2005(47):p.1498–1518.

[15.] Mac Donald, BJ. and Hashmi, MSJ., Analysis of Die Behaviour During Bulge Forming Operations Using The Finite Element Method. Finite Elements in Analysis and Design, 2002.39(2):p.137–51.

[16.] Mac Donald, B.J. and Hashmi, M.S.J., Finite Element Simulation of Bulge Forming Of a Cross-Joint From A Tubular Blank. J. Mater. Process. Technol, 2000.103(3):p.333–342.
[17.] Mac Donald, B.J., Non-Linear Finite Element Simulation of Complex Bulge Forming Processes. Ph.D. Thesis Dublin City University, 2000.
[18.] Teng, .G., Hu, Y.M., Behaviour of FRP-jacketed circular steel tubes and cylindrical shells under axial compression. Construction and Building Materials 21 (2007) 827–838.

[19.] Batika, M., Chen, J.F., Rotter, J.M., Teng, J.G.. Strengthening metallic cylindrical shells against elephant's foot buckling with FRP. Thin-Walled Structures 47(2009)1078–1091.

How to Cite This Article

Jafarpour, V., M. Abasi, Optimization of load values in pipe hydroforming process using fuzzy load control algorithm, 3(2022), 4683.https://doi.org/10.36937/ben.2022.4683